INTERNATIONAL JOURNAL OF ACADEMIC RESEARCH IN BUSINESS & SOCIAL SCIENCES

14, Issue 12, (2024) E-ISSN: 2222-6990

Performance Analysis of Class E ZVS Inverters Under Varying Load Conditions in APT Transmitter Units

Huzaimah Husin[1], ShakirSaat[1] , Yusmarnita Yusop[1] and Norezmi Jamal[2]

Center for Telecommunication Research & Innovation (CeTRI), Fakulti Kejuruteraan Elektronik dan Kejuruteraan Komputer, Universiti Teknikal Malaysia Melaka, 76100 Durian Tunggal, Melaka,Malaysia[1], Jabatan Teknologi Kejuruteraan Elektrik, Fakulti Teknologi Kejuruteraan, Universiti Tun Hussein Onn Malaysia, Hab Pendidikan Tinggi Pagoh, 84600 Panchor, Johor, Malaysia[2]

To Link this Article: http://dx.doi.org/10.6007/IJARBSS/v14-i12/23978 DOI:10.6007/IJARBSS/v14-i12/23978

Published Date: 29 December 2024

Abstract

This paper presents the design and analysis of a Class E Zero Voltage Switching (ZVS) inverter used in a 2.0 W Acoustic Power Transfer (APT) transmitter unit. The Class E ZVS inverter is chosen for its high-efficiency performance as an AC supply input voltage for an air transducer in an efficient acoustic power transfer system. The performance of the inverter under varying load conditions; resistive and actual air transducer modeled using the Butterworth Van-Dyke (BVD) equivalent circuit is investigated. The inverter is precisely designed to operate at the resonant frequency of 39.8 kHz, corresponding to the 40 kHz air transducer. Experimental results demonstrate a DC-AC power conversion efficiency of 85.42% with a resistive load. This study provides insights into the behaviour of the Class E ZVS inverter under different load conditions and suggests enhancements to improve efficiency in future applications.

Keywords: Class E Zvs Inverter, Acoustic Power Transfer, Π1a Impedance Matching, 40khz Air Transducer

Introduction

Pioneer open demonstration of wireless power transfer (WPT) was presented by Nikola Tesla in 1921 whereby the system managed to turn on an electric bulb using capacitor plates (Tesla, 1891). Unfortunately, even he managed to provide sufficient proof for WPT to become an alternative method in energy transfer, only after 1980, WPT started to get appropriate attention from researchers. The widely practiced and commercially available is Inductive Power Transfer (IPT) (Du et al., 2018) and (Zhang et al., 2019). One of the promising works in (Wang et al., 2022) shown 66.7% system efficiency with 10W load power was proposed at 2.5-meter IPT system for state detection equipment. However, the efficiency of IPT is often

compromised by metal surroundings and the physical dimensions of the coils used (Marques et al., 2022) and also the misalignment between transmitting and receiving coils (Luo et al., 2022). Another different established method compared to IPT is Capacitive Power Transfer (CPT) technique. Based on (Nabila et al., 2019), (Yusop et al., 2019) and (Paolucci et al., 2019), CPT offered less design complexity, which inherently can penetrate through any metal shielding environment. Apart from that, the CPT is also cheaper to construct and with possibility of a flexible design of the coupling plate. The main limitation of CPT technology is the inverse property of the capacitance with the distance, requiring high voltages and frequencies for the transfer of a certain amount of energy. However, CPT still can be a choice for short distance (<1mm) that can achieve high power (>1kW) transfer with reasonable efficiency as reported in (Yusop et al., 2019) and (Zhu et al., 2019). So, in order to overcome the major drawback of previous methods, Acoustic power transfer (APT) can be a choice due to its nature phenomena. As stated in (Roes et al., 2011), (Roes et al., 2013), (Husin et al., 2016), (Yuan et al., 2017), (Basaeri et al., 2019) and (Meesala et al., 2020), APT transfers power wirelessly by propagating energy as sound or vibration waves. Commonly, in order to transmit and receive the energy acoustically, air transducer that applied piezoelectricity conversion is practiced. The air transducer at the transmitter unit is typically excited using a power amplifier before transmitting energy through the propagation medium.

APT demonstrated its potential in 1985, with rapid development proving its suitability for in-body implantable devices. APT is a promising candidate for future WPT, particularly in biomedical applications and metal/non-metal environment surroundings (Yuan et al., 2017). Figure 1 illustrates APT technology, consisting of a transmitter and receiver unit. The transmitter generates acoustic energy at specific frequencies, while the receiver converts it back to electrical energy (Zaid et al., 2014). The transmission medium in APT can be any material that permits the propagation of pressure wave can be used. Till recent, APT gain a huge attention due to its safest WPT especially in biomedical implantable devices, data transfer, and through-wall transmission as reported in (Awal et al., 2016), (Kim et al., 2020), (Liu et al., 2023), (Wang & Lu, 2023), and and (Zheng et al., 2024). There are various driving circuits exist to drive air transducer with sinusoidal signals (Yuan et al., 2017), (Liu et al., 2023), (Siddiqui & Khan, 2019) and (You & Choi, 2020), the Class E ZVS resonant inverter is among the most practical to apply.

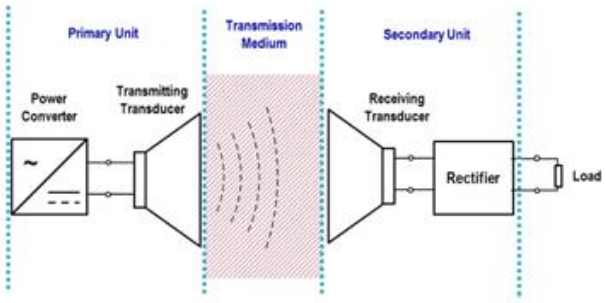

Figure 1 Basic diagram of APT technology (Zaid et al., 2014).

In the reports (Kazimierczuk, 2014), (Kazimierczuk & Czarkowski, 2012), (Hasan et al., 2021) and (Komanaka et al., 2022), the well-known reputable Class E ZVS inverter has been used as power amplifier to obtain high dc-ac power conversion efficiency. However, the effects of

parameter variations will interrupt the efficiency of power conversion of Class E ZVS inverter respectively as discussed in (Raab, 1978) and (Zhang & Ngo, 2021). The overall efficiency of each unit should be designed with a design efficiency of over 80% as suggested in (Ozeri & Shmilovitz, 2010) and (Taalla et al., 2019). In this work, the design of 2.0 W Class E ZVS inverter integrated with resistive component to represent the real part of air transducer total impedance is proposed as fundamental design stage, to in line with the nature of operating principle of Class E (Kazimierczuk, 2014) and (Hasan et al., 2021). In practical energy transmission applications, attaching an actual air transducer is required to observe the performance of the Class E ZVS inverter.

The nearest findings in APT based on Class E ZVS inverter were done by (Yuan et al., 2017). The work is driving air transducer directly based on actual air transducer equivalent circuit by departing from standard practices of Class E ZVS inverter which is optimized under purely resistive load. Furthermore, the researcher is more focused on different driving frequency rather than accomplishment of ZVS requirement. This article provides a step-by-step design process for Class E ZVS inverters, demonstrating their behaviour in real system conditions by changing the resistive component to an actual air transducer.

The significant contributions of the paper can be summarized as follows:

(i) The design of an APT transmitter unit that incorporated Class E ZVS inverter with actual 40 kHz air transducer.

(ii) The study of Class E ZVS inverter behaviour in different load resistance representations i.e. resistive component (fixed resistor) and complex impedance (actual transducer) has been made here. To date, to our knowledge, no results reported in this framework.

This paper discusses the APT technology system, research method, results and analysis, and proposed technique to overcome performance efficiency interruptions. It covers the theoretical calculation of Class E ZVS inverter and air transducer parameters, simulation results, experimental results, and actual air transducer behaviour. The study also demonstrates learning Class E ZVS inverter behaviour for different load representations at the APT transmitter unit.

Research Methodology

This section overviews the research methodology as illustrated in Figure 2.

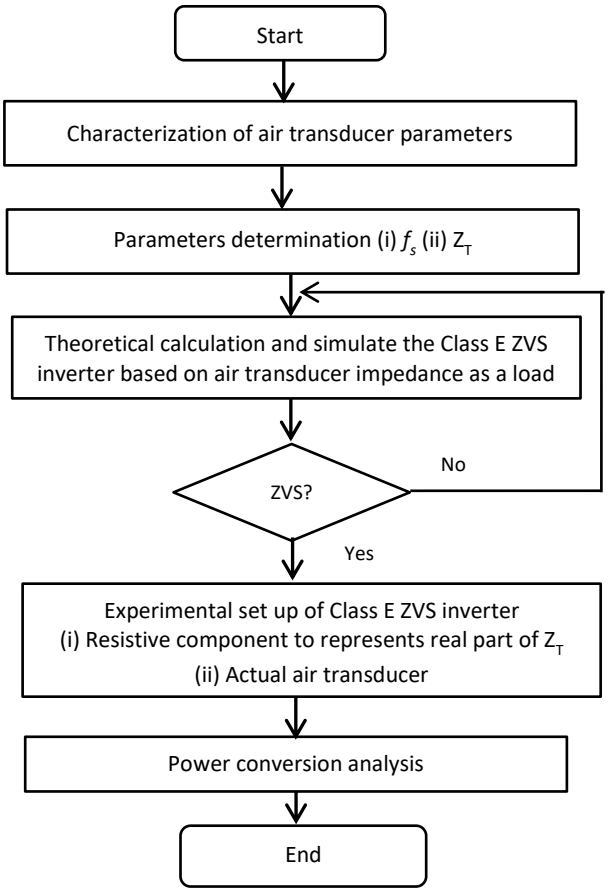

Figure 2: Methodology of the design process

Characterization of Air Transducer

The air transducer acts as a load in the Class E ZVS inverter for this paper. The Butterwoth Van Dyke (BVD) model as in (Yuan et al., 2017) and (Arnold & Martins, 2020) used to model air transducer 40 kHz MCUSR18A40B12RS from Multicomp. The model is shown in Figure 3 describes the mechanical part (R_1, L_1 and C_1) and the electrical part (the clamping capacitor) (C_0) of the air transducer.

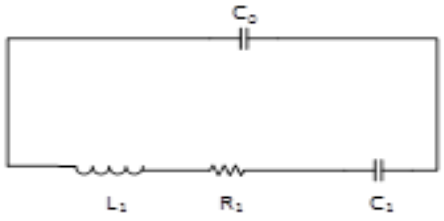

Figure 3: BVD model for air transducer (Siddiqui & Khan, 2019)

The parameters of air transducer are determined using Keysight E4990A Impedance Analyzer. The Table 1 tabulates the parameters of air transducer based on BVD model.

Table 1
Parameters of BVD Model for Air Transducer

$R_1(\Omega)$	$L_1(H)$	$C_1(F)$	$C_0(F)$
482.36	109.70m	144.60p	1.94n

From the parameter of BVD model for air transducer, the total impedance of the air transducer can be expressed as:

$$Z_T = \frac{\left(R_1 + j\omega L_1 + \frac{1}{j\omega C_1}\right).\frac{1}{j\omega C_0}}{R_1 + j\omega L_1 + \frac{1}{j\omega C_1} + \frac{1}{j\omega C_0}} \quad (1)$$

From Equation (1), the air transducer will exhibit the series resonant frequency and can be calculated as in Equation 2.

$$f_{series} = \frac{1}{2\pi\sqrt{L_1 C_1}} \quad (2)$$

Then from Equation (1), the real part of total impedance, for air transducer used for this works is 469.7Ω, meanwhile the series resonant frequency, is 39.8 kHz respectively. The nature of Class E ZVS inverter requires the resistive load, so it can perform at the optimum operation region (Kazimierczuk, 2014). Thus, in this paper, the work considers only the real part of air transducer impedance, so that the load value, R for a Class E ZVS inverter is rounded to 470 Ω, and the switching frequency is chosen based on a series resonant frequency which is 39.8 kHz.

Class E ZVS inverter theoretical calculations

Class E ZVS inverter is well known as a high efficiency resonant inverter that capable to operate at the frequencies of kHz to MHz and, is shown in Figure 4 consists of a DC signal source; Vcc, a power MOSFET that operates as a switch, a choke inductor; Lchoke, a shunt capacitor; Cs, and a L-C-R series resonant circuit.

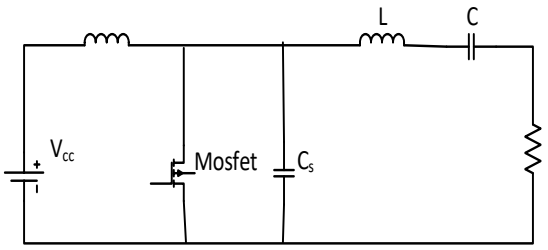

Figure 4: A single-ended Class E ZVS inverter (Kazimierczuk, 2014),

The driving signal, is the square wave control signal with the duty ratio, D, to control the on and off condition of power MOSFET. The power MOSFET is capable of ensuring zero switching losses during switching time intervals, resulting in a high efficiency inverter (Kazimierczuk & Czarkowski, 2012). The ZVS condition demands that the switch voltage (V_{DS}) at the instant the switch (V_{GS}) is turned on should be zero and can be described in Figure 5.

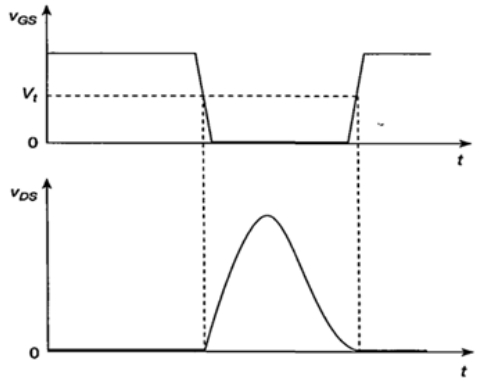

Figure 5: Waveforms of VGS versus VDS in Class E ZVS inverter operation (Kazimierczuk, 2014)

The design process of Class E ZVS inverter is carried out with few assumptions such as stated in (Kazimierczuk, 2014) for this paper.

i. Power output intended, Pout = 0.7 W
ii. Loaded quality factor, Q = 10
iii. Static Drain-to-Source resistance, rDS = 0.54 Ω
iv. Duty cycle, D = 0.5

Design process followed by the calculation of the circuit parameters of Class E ZVS inverter using established equations in (Kazimierczuk, 2014). The DC signal source, VDC, can be determined based on our desired output power and dedicated load resistance using;

$$V_{DC} = \sqrt{\frac{R[P_o(\pi^2+4)]}{8}} \tag{3}$$

The choke inductor, L_{choke} for the circuit is calculated as;

$$L_{choke} = 2\left(\frac{\pi^2}{4}+1\right)\frac{R}{f_s} \tag{4}$$

In order to determine the value of shunt capacitor, C_s, the following equation can be applied.

$$C_s = \frac{8}{\pi(\pi^2+4)\omega R} \tag{5}$$

The series resonant network L-C can be calculated by

$$L = \frac{QR}{\omega} \tag{6}$$

$$C = \frac{1}{\omega R\left[Q - \frac{\pi(\pi^2-4)}{16}\right]} \tag{7}$$

The value of output voltage generated at the load, is calculated as:

$$V_{R(max)} = V_{DC}\frac{4}{\sqrt{\pi^2+4}} \quad (8)$$

The selection of power MOSFET is regards to the maximum operating voltage and power dissipation allowable in the datasheet. Therefore, the maximum switching voltage produced by the circuit can be calculated by:

$$V_{DS(Max)=}3.562V_{DC} \quad (9)$$

In order to compare the power conversion efficiency, the input power of the circuit can be obtained using:

$$P_{input} = V_{DC}I_{dc} \quad (10)$$

Meanwhile, I_{dc} is similar to current through the choke inductor, I_{Lf} and can be calculated as:

$$I_{Lf} = \left(\frac{8}{\pi^2+4}\right)\frac{V_{DC}}{R} \quad (11)$$

As a result, from Equation 12, we can get the current through the resistor as follow:

$$I_{R(\max)} = \left(\frac{\sqrt{\pi^2+4}}{2}\right)I_{Lf} \quad (12)$$

The objective of this particular work is to determine the power converted by the Class E ZVS inverter, thus the output power for resistive load at the transmitting transducer can be determined by;

$$P_{output} = \frac{\left(V_{R(rms)}\right)^2}{R} \quad (13)$$

As overall comparison, the efficiency of the inverter will be justified using;

$$\eta = \frac{P_{output}}{P_{input}} \quad (14)$$

By applying Equations 1-14, the calculated value of each component and parameters in the 2.0 W Class E ZVS inverter is presented in Table 2.

Table 2
Calculated Value for Class E ZVS Inverter

Inverter Parameters	**Symbol**	**Value**	**Unit**
Load	R_s	47.252	Ω
Series resonance frequency	f_s	39.8	kHz
DC voltage supply	V_{DC}	12.8	V
Choke inductor	L_f	8300	µH
Shunt capacitor	C_s	17	nF
Series inductor	L	966.49	µH
Series capacitor	C	22.09	nF
Voltage across the load resistance	$V_{R(peak)}$	13.72	V
Voltage across the switch	V_{DS}	45.49	V
Input power	P_{input}	2.0	W
Input current	I_{dc}	157.0	mA
Output current across the load	$I_{R(peak)}$	29.2	mA
Output power	P_{output}	2.0	W
Efficiency	η	100	%

Results and Analysis

Class E ZVS inverter simulation design
The Class E ZVS inverter is designed using equation values in Table 2, and verified using Pspice software, aiming for a waveform and desired output power of 2.0 W, as illustrated in Figure 6.

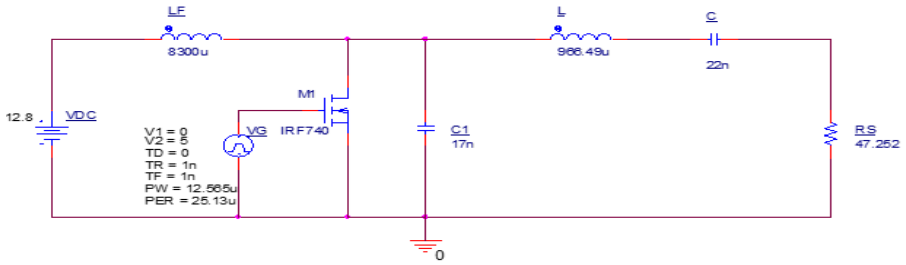

Figure 6: The simulation diagram of 2.0 W Class E ZVS inverter design
In this section, the accomplishment of ZVS waveform is shown in Figure 7. It can be observed that the switch voltage (V_{DS}) at the instant the switch (V_{GS}) is turned on is zero as proposed in (Kazimierczuk, 2014) which is called as nominal waveform of V_{DS}. This to ensure the inverter managed to convert the supplied dc voltage to ac voltage for further consumption of air transducer effectively.

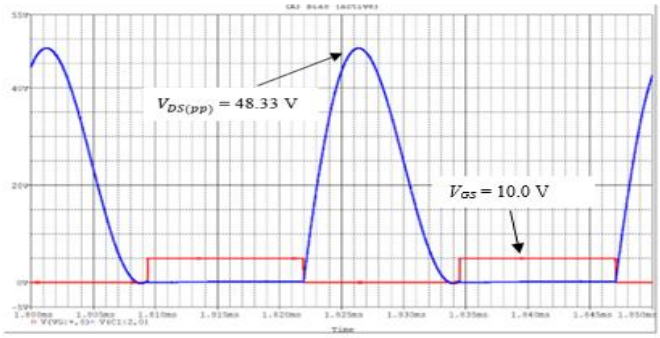

Figure 7: The ZVS waveform simulation result

It is highly recommended the tuning process must be simultaneously fulfil the two desired conditions: nominal waveform of and the desired output power, that being produced at the load, in which 2.0 W in the work. For the simulation results, the input power, and output power, waveforms are depicted in Figure 8a and Figure 8b, respectively. Based on Figure 8a, 153 mA is produced as input current, for the inverter with the direct voltage supplied, is maintained at 12.8 V. Thus, based on these values, the calculated input power, is P_{input}= 153mA x 12.8V = 1.96 W as in Equation 10. Based on Figure 8a, 153 mA is produced as input current, for the inverter with the direct voltage supplied, is maintained at 12.8 V. Thus, based on these values, the calculated input power, is x= 153mA x 12.8V = 1.96 W as in Equation 10. In order to determine the efficiency, η of the dc-to-ac power conversion, the output power, that developed at the load must also being verified. Figure 8b shows the values of output voltage and current correspondingly. The simulation approach produced output voltage, as 9.57V_{rms} and output current, as 109.0 mA_{pp}.

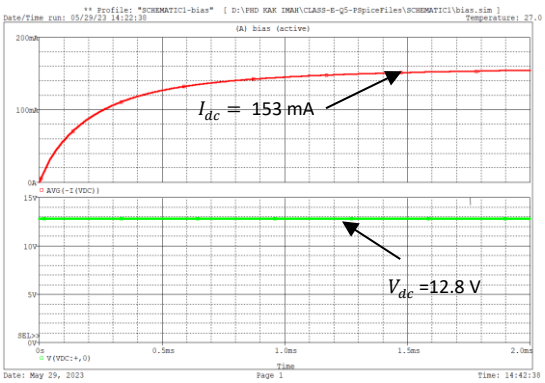

(a) The input current and voltage simulation result

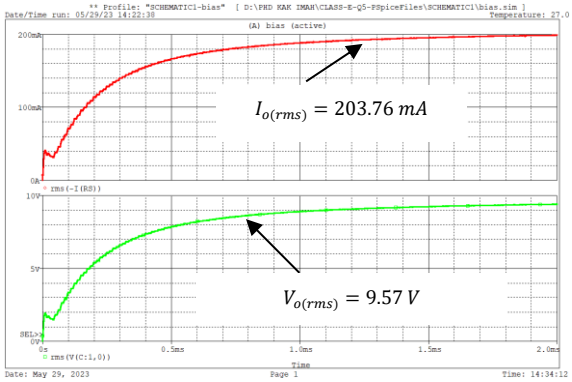

(b) The output current and voltage simulation result

Figure 8: Input and output power simulation results

Using Equation 13, $V_{output(rms)}$ is being divided by the real value of air transducer total impedance, 470 Ω and the output power, P_{output} it becomes 1.94W. The high efficiency, η, which is 98.0% of Class E ZVS inverter is viable through the Pspice Simulation alteration in this work. The efficiency, η in this work that converting the dc-to-ac power was calculated using Equation 15.

Class E ZVS inverter experimental results

The capability of Class E ZVS inverter to excite the air transducer as a load at the transmitter unit is being investigated. The dc supplied, 12.8 V for Class E Inverter and the input supply (10Vpp with 39.8 kHz) for the MOSFET driver, TC4422 are provided by ED-4770 Combo Tester. The measurements of voltage and phase angle are taken using Keysight Digital Storage Oscilloscope DSO-X-2012A and for the current measurement, Keysight Current Probe and Keysight N2279A Power Supply for current probe are used. The investigation is being carried out in two sub-sections to evaluate performance of proposed Class E ZVS inverter; (1) air transducer modeled as resistive load and (2) air transducers as in equivalent circuit which consists of resistance and reactance components based on BVD model approach. All the previous calculation value for Class E ZVS inverter remains unchanged. The aim of this section is to compare the performance of proposed Class E ZVS inverter for different load resistance representations.

Resistive representation

Figure 9 illustrates the experimental set up for the 2.0 W Class E ZVS inverter for resistive air transducer representation. The setup consists of a DC power source, and two digital oscilloscopes to measure two key parameters, i.e., ZVS waveform and output power that were produced by the Class E ZVS inverter in this work. Apart from that, the oscilloscope was also applied to generate the sinusoidal waveform that purposely drives the MOSFET as the switching device in the circuit. The 39.8 kHz sinusoidal waveform that supplied to the MOSFET has a same value in frequency as the resonant frequency of the air transducer that was applied as the transmitting device in the APT transmitter unit.

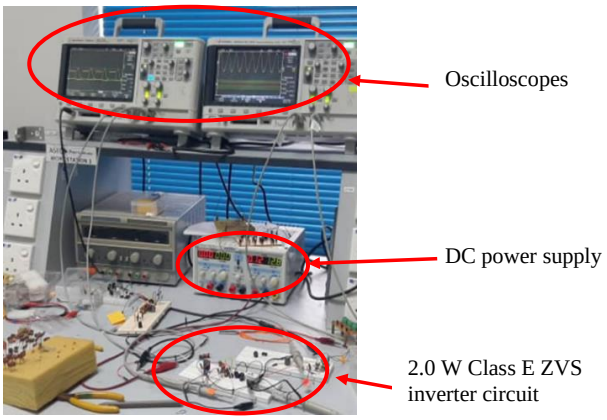

Figure 9: The complete 2.0 W Class E ZVS inverter experimental setup

The ZVS condition was being observed and portrayed in Figure 5, was fulfilled as illustrated in Figure 10. The input power, for this experimental set up is Vcc x Idc = 12.8V x 150mA = 1.92W and shown in Figure 11a. Based on Figure 11b, the peak-to-peak output voltage of 24.9V or in the rms value as 8.80V, and by using Equation 13, $V_{output(rms)}$ is being divided by the real value of air transducer total impedance of 470 Ω, in which produces 1.64 W as it output power, . Thus, the efficiency of Class E ZVS inverter under resistive load experimental setup is 85.42%, considered as acceptable for the inverter performance efficiency.

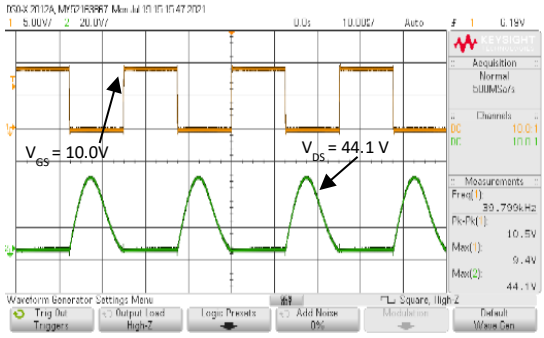

Figure 10: The ZVS waveform experimental result

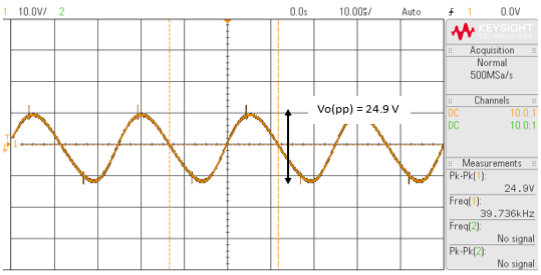

(a) The input current and voltage experimental result (b) The output voltage experimental result

Figure 11: Input and output power experiment results

The tradeoff between nominal waveform of VDS and desired output power at the load makes the tuning process quite challenging and thus limiting the efficiency in the experimental setup compared to simulation results. Furthermore, the components used in the circuit may not 100% purely resistive, inductive or capacitive that also contributes to the efficiency reduction, from 98.97% in simulation results to 85.42% in experimental results.

Actual air transducer device

The actual marketable 40 kHz air transducer, MCUSR18A40B12RS from Multicomp, is attached as a load with the Class E ZVS inverter. The circuit in which air transducer is being excited by the Class E ZVS inverter as shown in Figure 12.

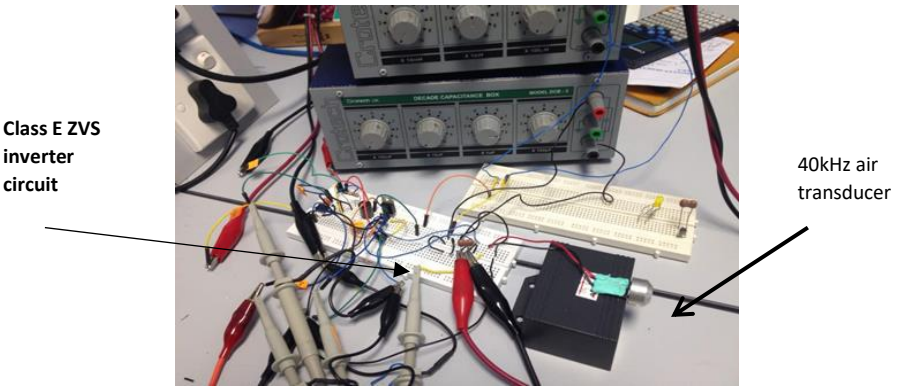

Figure 12: 2.0 W Class E ZVS inverter with 40 kHz air transducer

In this section, the 470 Ω resistive component that imitated only the real part value of total transducer impedance, is changed to the actual air transducer that consists of complex impedance. The disruption can be clearly observed in Figure 13, whereby these two waveforms overlap significantly, whereby both the voltage the instant the switch, and the switch voltage, are simultaneously active, which could lead to increased power losses. It means that the requirement of having zero voltage for MOSFET at the transistor's turn-on time as recommended is not accomplished. Even though the nominal waveform of ZVS is heavily interrupted, the work demonstrated that the switching voltage, is equal to 47 V, which is almost three times greater than DC supply voltage, and is maintained at 10.0 V respectively, remaining still in line with the theoretical. The designed Class E ZVS inverter also managed to maintain the desired operating frequency at 39.8 kHz as required.

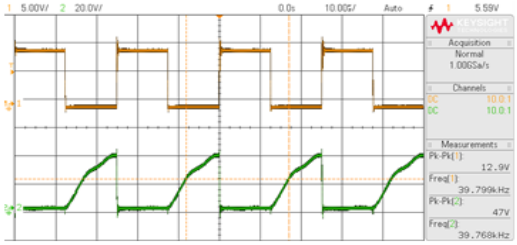

Figure 13: The ZVS waveform experimental result

Figure 14(a) displays the Class E ZVS inverter input current, and voltage, which contributed to the very low input power, of 384 mW compared to the required of 2.0 W. The relationship between the input current, that is proportionally inverse with load, R can be seen in Equation 11.

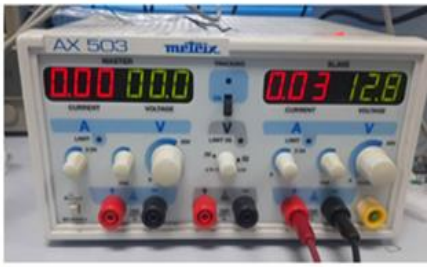

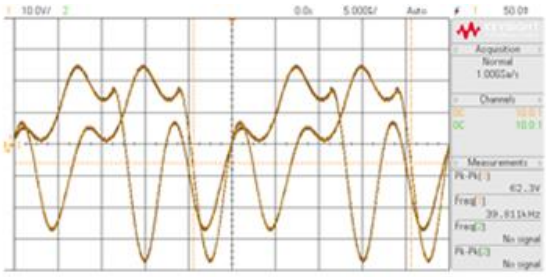

(a) the input current and voltage (b) the output voltage

Figure 14: Experimental results of 2.0 W Class E ZVS inverter with 40 kHz air transducer

Meanwhile, in Figure 14(b), the waveform of output voltage displayed significant variations in amplitudes, which indicates the instability and inefficiency in the power conversion process. When a circuit that originally only had a resistive load (which produces a clean sinusoidal wave with no harmonics) is converted to an RC load, the capacitor's response to voltage changes causes the waveform to become more complex. The uneven amplitude may be caused by the charging and discharging process of the capacitor in the circuit. The efficiency of Class E ZVS inverter in this particular section cannot be determined due to the off-nominal waveform and desired input power, produced at the load is far less from the design specification. This occurred due to the load mismatch in these two designs. The Class E ZVS inverter's high efficiency can be recovered by equipping it with a matching circuit that provides an impedance matching network.

Proposed Design Enhancement

As the nature of Class E ZVS inverter that sensitive to load variations, it is suggested to equip the inverter with the matching network that provides impedance transformation, such as π1a or π1b circuit as discussed in This solution transforms the load into desired ones and maintains the input voltage to the transmitting transducer within the applied load ranges. In APT transmitter unit, the highest vibration energy is generated while the air transducer in the series mode resonant. In this mode, the air transducer as in Figure 4, can be modelled using the BVD approach and it becomes circuit that only consists of C0 that parallel with R1. Once the Class E ZVS inverter and the model are combined, it creates a topology similar with π1a impedance matching technique. This particular arrangement of air transducer will be performed as impedance matching circuit for the Class E ZVS inverter as displayed in Figure 15.

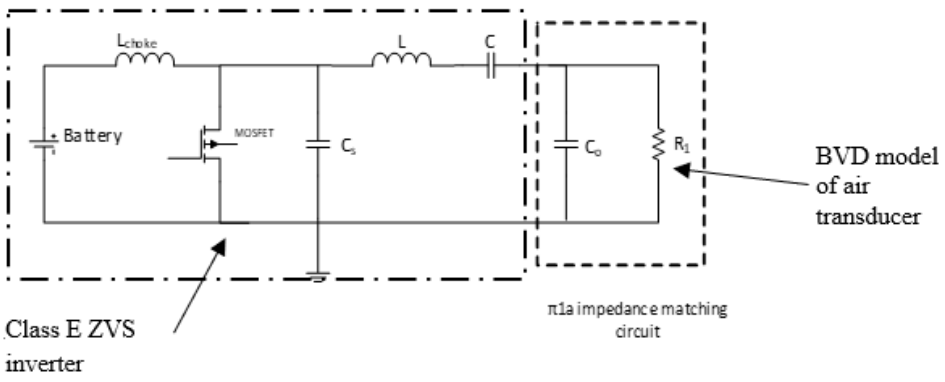

Figure 15: Suggested Class E ZVS inverter with π1a matching network for future design

Conclusion and Future Work

This study contributes significantly to the existing body of knowledge on Class E ZVS inverters by systematically analysing their behaviour under varying load conditions, including complex impedance represented by an actual 40 kHz air transducer modeled via the Butterworth Van Dyke (BVD) circuit. Theoretically, it expands the understanding of inverter efficiency disruptions caused by load variations, a critical aspect often overlooked in practical implementations. Contextually, the findings are highly relevant to Acoustic Power Transfer (APT) systems, particularly for applications requiring reliable and efficient wireless power delivery, such as biomedical implants and through-wall energy transmission. By addressing load sensitivity issues and proposing impedance matching enhancements using π1a network, this research bridges the gap between idealized inverter performance and real-world conditions, paving the way for more robust and efficient APT transmitter units.

Acknowledgement

The authors would like to thank the Ministry of Higher Education of Malaysia for their support through research grant FRGS/1/2023/TK07/UTEM/02/3 and the support facilities from Advanced Sensor and Embedded Control Systems Research Group (ASECs), FTKEK, Universiti Teknikal Malaysia Melaka (UTeM).

References

Arnold, F. J., & Martins, P. S. (2020). New insights into the mechanical pre-stressing of piezotransducers. Journal of Intelligent Material Systems and Structures, 32(8), 867–879. https://doi.org/10.1177/1045389x20974436

Awal, R., Jusoh, M., Sabapathy, T., Kamarudin, M. R., & Rahim, R. A. (2016). State-of-the-Art Developments of Acoustic Energy Transfer. International Journal of Antennas and Propagation, 2016, 1–14. https://doi.org/10.1155/2016/3072528

Basaeri, H., Yu, Y., Young, D., & Roundy, S. (2019). Acoustic power transfer for biomedical implants using piezoelectric receivers: Effects of misalignment and misorientation. Journal of Micromechanics and Microengineering, 29(8), 084004–084004. https://doi.org/10.1088/1361-6439/ab257f

Du, S., Chan, E., Bing, W., Hong, J., Widmer, H., & Wheatley, C. E. (2018). Wireless Power Transfer Using Oscillating Magnets. IEEE Transactions on Industrial Electronics, 65(8), 6259–6269. https://doi.org/10.1109/tie.2017.2786289

Hasan, K. K., Saat, S., Yusop, Y., Husin, H., & Sin, N. D. M. (2021). The design of an efficient class E-LCCL capacitive power transfer system through frequency tuning method. International Journal of Electrical and Computer Engineering (IJECE), 11(2), 1095. https://doi.org/10.11591/ijece.v11i2.pp1095-1104

Husin, S. H., Md Saat, M. S., Yusop, Y., Abdul Ghani, Z., & Nguang, S. K. (2016). Development of Class D Inverter for Acoustics Energy Transfer Implantable Devices. International Journal of Power Electronics and Drive Systems (IJPEDS, 7(1), 75. https://doi.org/10.11591/ijpeds.v7.i1.pp75-84

Kazimierczuk, M. K. (2014). RF Power Amplifiers. John Wiley & Sons.

Kazimierczuk, M. K., & Czarkowski, D. (2012). Resonant Power Converters. John Wiley & Sons.

Kim, J., Kim, K., Choe, S.-H., & Choi, H. (2020). Development of an Accurate Resonant Frequency Controlled Wire Ultrasound Surgical Instrument. Sensors, 20(11), 3059–3059. https://doi.org/10.3390/s20113059

Komanaka, A., Zhu, W., Wei, X., Nguyen, K., & Sekiya, H. (2022). Load-independent inverse class-E ZVS inverter and its application to wireless power transfer systems. IET Power Electronics, 15(7), 644–658. https://doi.org/10.1049/pel2.12256

Liu, W., Chau, K. T., Tian, X., Wang, H., & Hua, Z. (2023). Smart wireless power transfer — opportunities and challenges. Renewable and Sustainable Energy Reviews, 180, 113298. https://doi.org/10.1016/j.rser.2023.113298

Luo, T., Zhang, S., & Zhou, F. (2022). Research on an Underwater Inductive Coupling Power Transfer Method. 2022 IEEE 4th International Conference on Power, Intelligent Computing and Systems (ICPICS), 167–173. https://doi.org/10.1109/icpics55264.2022.9873779

Marques, E. G., Mendes, M. M., & Costa, V. S. (2022). Inductive Power Transfer: Past, Current, and Future Research. IntechOpen EBooks. https://doi.org/10.5772/intechopen.108484

Meesala, V. C., Hajj, M. R., & Shahab, S. (2020). Analysis and prediction of shock formation in acoustic energy transfer systems. Journal of Applied Physics, 128(23), 234902. https://doi.org/10.1063/5.0026645

Nabila, N., Saat, S., Yusop, Y., Isa, M. S. M., & Basari, A. A. (2019). The design of auto-tuning capacitive power transfer for rotary applications using phased-locked-loop. International Journal of Power Electronics and Drive Systems (IJPEDS, 10(1), 307–307. https://doi.org/10.11591/ijpeds.v10.i1.pp307-318

Ozeri, S., & Shmilovitz, D. (2010). Ultrasonic transcutaneous energy transfer for powering implanted devices. Ultrasonics, 50(6), 556–566. https://doi.org/10.1016/j.ultras.2009.11.004

Paolucci, T., Pezzi, L., Centra, M., Porreca, A., Barbato, C., Bellomo, R., & Saggini, R. (2019). Effects of capacitive and resistive electric transfer therapy in patients with painful shoulder impingement syndrome: A comparative study. Journal of International Medical Research, 48(2), 030006051988309. https://doi.org/10.1177/0300060519883090

Raab, F. H. (1978). Effects of circuit variations on the class E tuned power amplifier. IEEE Journal of Solid-State Circuits, 13(2), 239–247. https://doi.org/10.1109/jssc.1978.1051026

Roes, L., Duarte, J. L., Hendrix, M. A. M., & Lomonova, E. A. (2013). Acoustic Energy Transfer: A Review. IEEE Transactions on Industrial Electronics, 60(1), 242–248. https://doi.org/10.1109/tie.2012.2202362

Roes, L., Hendrix, M., & Duarte, J. L. (2011). Contactless energy transfer through air by means of ultrasound. IECON 2020: The 46th Annual Conference of the IEEE Industrial Electronics Society. https://doi.org/10.1109/iecon.2011.6119486

Siddiqui, A., & Khan, A. (2019). Mechanism and Optimization of Acoustic Power Transfer Systems. 2019 International Conference on Power Electronics, Control and Automation (ICPECA). https://doi.org/10.1109/icpeca47973.2019.8975391

Taalla, R. V., Arefin, Md. S., Kaynak, A., & Kouzani, A. Z. (2019). A Review on Miniaturized Ultrasonic Wireless Power Transfer to Implantable Medical Devices. IEEE Access, 7, 2092–2106. https://doi.org/10.1109/access.2018.2886780

Tesla, N. (1891). Experiments with Alternate Currents of Very High Frequency and their Application to Methods of Artificial Illumination. Transactions of the American Institute of Electrical Engineers, VIII(1), 266–319. https://doi.org/10.1109/t-aiee.1891.5570149

Wang, X., & Lu, M. (2023). Wireless power transmission based on retro-reflective beamforming technique. Space Solar Power and Wireless Transmission. https://doi.org/10.1016/j.sspwt.2023.08.001

Wang, Y., Liu, Z., Gu, P., & Xu, D. (2022). Analysis and Design of a Wide Air Gap IPT System with Multi-Load CV Characteristics Based on Cylindrical Solenoid Coupler. 2022 International Power Electronics Conference (IPEC-Himeji 2022- ECCE Asia). https://doi.org/10.23919/ipec-himeji2022-ecce53331.2022.9807227

You, K., & Choi, H. (2020). Inter-Stage Output Voltage Amplitude Improvement Circuit Integrated with Class-B Transmit Voltage Amplifier for Mobile Ultrasound Machines. Sensors, 20(21), 6244. https://doi.org/10.3390/s20216244

Yuan, T., Dong, X., Shekhani, H., Li, C., Maida, Y., Tou, T., & Uchino, K. (2017). Driving an inductive piezoelectric transducer with class E inverter. Sensors and Actuators A: Physical, 261, 219–227. https://doi.org/10.1016/j.sna.2017.05.021

Yusop, Y., Saat, S., Ghani, Z., Husin, H., M. K., A., & Kiong Nguang, S. (2019). Cascaded Boost-Class-E for rotary capacitive power transfer system. The Journal of Engineering, 2019(17), 3742–3748. https://doi.org/10.1049/joe.2018.8016

Zaid, T., Saat, S., Yusop, Y., & Jamal, N. (2014). Contactless energy transfer using acoustic approach - A review. 2014 International Conference on Computer, Communications, and Control Technology. https://doi.org/10.1109/i4ct.2014.6914209

Zhang, H., Chen, Y., Park, S.-J., & Kim, D.-H. (2019). A Hybrid Compensation Topology with Single Switch for Battery Charging of Inductive Power Transfer Systems. IEEE Access, 7, 171095–171104. https://doi.org/10.1109/access.2019.2955805

Zhang, L., & Ngo, K. (2021). A Constant-Current ZVS Class-E Inverter With Finite Input Inductance. IEEE Transactions on Industrial Electronics, 68(8), 7693–7696. https://doi.org/10.1109/tie.2020.2998764

Zheng, Y., Zhang, Z., Zhang, Y., Pan, Q., Yan, X., Li, X., & Yang, Z. (2024). Enhancing Ultrasound Power Transfer: Efficiency, Acoustics, and Future Directions. Advanced Materials. https://doi.org/10.1002/adma.202407395

Zhu, Q., Zang, S., Zou, L. J., Zhang, G., Su, M., & Hu, A. P. (2019). Study of coupling configurations of capacitive power transfer system with four metal plates. Wireless Power Transfer, 6(2), 97–112. https://doi.org/10.1017/wpt.2019.10